DOE/ER/45390--3

DE92 015198

SYNOPSIS

This report summarizes the results of a study of the relationship between microstructure and magnetic properties in a unique genre of ferromagnetic material characterized by a polysynthetically twinned structure which arises during solid state transformation. These results stem from the work over a period of approximately 27 months of a nominal 3 year grant period. The report also contains a proposal to extend the research project for an additional 3 years.

The polytwinned structures produce an inhomogeneous magnetic medium in which the easy axis of magnetization varies quasi-periodically giving rise to special domain configurations which are expected to markedly influence the mechanism of magnetization reversal and hysteresis behavior of these materials in bulk or thin films. The extraordinary permanent magnet properties exhibited by the well-known Co-Pt alloys as well as the Fe-Pt and Fe-Pd systems near the equiatomic composition derive from the formation of a polytwinned microstructure. The twinning arises from the cubic (A1) → tetragonal ($L1_o$) ordering transformation characteristic of these alloy systems. The polytwinned state in these high magnetocrystalline anisotropy (K ~ 10^7-10^8 ergs/cc) alloys is comprised of twin lamellae conjugated along the {110} planes of the parent cubic phase. This fine-scale twinning produces an interesting synergism between the "structural domains" (twins) and the magnetic domain structure. Numerous theoretical analyses of the twinned ferromagnets have suggested strongly that optimum magnetic properties have not yet been achieved in these materials and that a significant enhancement of the properties might be achieved through a better understanding of the relationship between the structure and the mechanism of coercivity. Importantly, although the Co-Pt, Fe-Pt and Fe-Pd alloys are not likely to find

DISCLAIMER

application as bulk permanent magnet materials there is great technological potential for this family of ferromagnets in special thin film applications e.g. integrated magnetic and semiconducting devices, and perhaps magnetic recording.

In this research program the magnetic hardening associated with the A1 → $L1_0$ transformation in the Fe-Pt and Fe-Pd permanent magnet alloys has been studied primarily using transmission electron microscopy (TEM/STEM), X-ray diffraction, Lorentz microscopy, and vibrating sample magnetometry (VSM). The initial period of research has been very fruitful and has indeed revealed a rich panorama of structure-property relationships in these polytwinned alloys. It has been established that the ordering reaction generally occurs via a nucleation and growth process strongly influenced by the transformation strain. The ordered nuclei exhibit a non-equilibrium c/a ratio and have a plate-like morphology lying along the {110} planes of the cubic matrix. The strain induced preferential growth and coarsening of the coherent, ordered precipitates gives rise to a redistribution of the three variants (c-axes) and particle alignment resulting in the formation of an interpenetrating banded structure and microtwins. After prolonged aging the polytwinned structures exhibit a "discontinuous coarsening" reaction similar to that observed in eutectoid or eutectic structures. Above all, it is clear from these new studies of the development of the polytwinned microstructures that the banded twin structure derives from a coalescence of growing individual particles having a common c-axis under the influence of the transformation strain. The coalescence often leads to the formation of antiphase boundaries (APB's) and these planar faults appear to act as obstacles to domain wall motion.

The evolution of the magnetic domain structure attendant to the transformation process has been characterized for the first time using Lorentz microscopy. These

preliminary results indicate that a magnetically modulated structure exists virtually throughout the course of the A1 → $L1_0$ transformation and the formation of the polytwinned structures. Peak hardness in both the Fe-Pt and Fe-Pd alloys appears to correspond to a state of complete order rather than a two-phase state comprised of ordered particles dispersed in a disordered matrix as suggested most often in the literature. A tentative model of the coercivity has been developed based on APB pinning taking into account the measured temperature dependence of the coercivity and experimentally observed domain wall behavior. This simple model includes a first approximation to account for the influence of thermally activated wall motion past the planar obstacles (APB's).

The initial stages of these studies has taken a preliminary look at the influence of microstructural refinement through rapid solidification on the resultant structure-properties relationships in the equiatomic Fe-Pd alloy. A decrease in the grain size and scale of the twinned structure appears to have doubled (250 to 500 Oe) the coercivity in the rapidly-solidified material compared to the bulk processed alloy. The microstructural term in the coercivity model related to the microtwin size and APB density is most likely responsible for this enhanced magnetic hardness. The fundamental basis for this result, however, will be a major focus of the future research program.

I. INTRODUCTION

Fe-Pt and Fe-Pd alloys can develop coercivities in the range H_c ~ 500 Oe to 5kOe and energy products $(BxH)_{max}$ ~ 5-20 MGOe. Both alloy systems derive their properties from CuAuI($L1_o$)-type ordering and the ordered tetragonal phase exhibits a uniaxial magnetocrystalline anisotropy ~ 2-7 x 10^7 erg/cc similar to the well-known Co-Pt alloy where K ~ 5 x 10^7 erg/cc [1,2]. The Fe-Pt, Fe-Pd and Co-Pt family is characterized by a polytwinned structure (see Figures 1a-d) which emerges during the A1 (disordered fcc) → $L1_o$ (ordered tetragonal) transformation to relax the strain energy attendant to the atomic ordering reaction [3,4]. The phase diagrams of the Fe-Pt and Fe-Pd systems are shown in Figure 2 and the first-order A1 → $L1_o$ transformation is evident in the vicinity of the equiatomic composition.

As pointed out in the works of Khachaturyan [5] and Roitburd [6] the underlying principles governing the evolution of the polytwinned state during the A1 → $L1_o$ solid state transformation characteristic of these alloys are essentially the same as those involved in the occurrence of structural domains (twins) in martensitic transformations and the occurrence of ferromagnetic domains (regions of spin alignment) in ferromagnets. In the case of a phase transformation in the solid state, the elastic misfit or strain energy attendant to atomic rearrangement is reduced by the mutual arrangement of the crystallographic variants or structural domains; ferromagnetic domains essentially arise from a reduction of the magnetostatic energy through mutual arrangement of the variants of the direction of magnetization. The polytwinned morphology associated with the order → disorder or martensitic transformations relaxes the bulk elastic strain energy because the multi-domain (structural domains) collapses the elastic field to a small region near the interface and

globally approximates an invariant plane strain. Of course, this occurs at the expense of a surface energy associated with the domain or twin boundaries. Similarly, ferromagnetic domain formation produces a large decrease in the magnetostatic energy of a ferromagnetic material (below some critical size) by effecting flux closure with an expenditure of surface energy associated with the Bloch walls in the multi-domain state. The Fe-Pt, Fe-Pd, and Co-Pt ferromagnets represent an unique synergism between structural domains and magnetic domains and an interesting realm for microengineering the properties of these materials.

The polytwinned nature of the high anisotropy $L1_o$-type ordered ferromagnets has often been ignored in the analysis of the origin of coercivity in these materials. For example, Gaunt [7] concluded that the coercivity of Co-Pt alloys stems from domain wall pinning produced by large gradients in domain wall energy within a fine mixture of the disordered cubic and ordered tetragonal phases emphasizing the need for coexisting ordered and disordered regions for high coercivity. In this model it is expected that the coercivity should drop-off rapidly as the fully ordered state is achieved. The role of the twin microstructure has been the focus of discussion of a number of investigators in the Soviet literature [8-10]. The unique hierarchy of possible domain configurations in these magnetically modulated ferromagnets has been clearly recognized and discussed. However, in spite of this interest in the magnetic structure of the polytwinned state surprisingly no definitive Lorentz microscopy studies were carried out to experimentally examine the magnetic domains. The early Soviet work did make a preliminary attempt to consider the salient microstructural features of the twinned alloys in terms of possible mechanisms of wall pinning in the completely ordered state including the effect of antiphase boundaries on magnetic properties

[11]. However, as emphasized in a more recent overview [12], the Soviet School has concluded that more theoretical and experimental work are required to elucidate the mechanisms of coercivity controlling magnetization reversal in these lamellar composites. This latter paper strongly suggested that the polytwinned ferromagnets have great potential for developing markedly enhanced properties through elucidation of the structure-property relationships governing magnetization reversal.

The goal of this research project sponsored by the Department of Energy is to comprehensively study the mechanism of the phase transformation and attendant twinning phenomena which govern the evolution of the polysynthetically twinned microstructures and magnetic domain structures in Fe-Pt and Fe-Pd based alloys leading to the extraordinary magnetic properties exhibited by these unique ferromagnets. The research is aimed at critically evaluating the relationship between the nature of the polytwinned structures and the fundamental mechanisms of magnetization reversal which govern the technical magnetic properties in terms of domain magnetics. A range of metallographic tools are being utilized to study the microstructural development including conventional transmission electron microscopy (TEM), analytical electron microscopy (AEM), atom probe field-ion microscopy (APFIM), and X-ray diffraction. Also, Lorentz microscopy studies are being employed to directly observe the fine-scale magnetic domain structures which develop in the polysynthetically twinned crystals.

II. SUMMARY OF RESULTS

A. Transformation Behavior and the Development of the Polytwinned Structures

According to the X-ray and electron diffraction results, the as-quenched and as-melt-spun Fe-Pd alloys were disordered exhibiting the expected face-centered cubic (fcc) structure; however, the as-quenched Fe-Pt alloys were generally characterized by a fine dispersion of small ordered particles ($L1_o$) embedded in a disordered fcc matrix. The critical temperature T_c for ordering ($A1 \rightarrow L1_o$) in the Fe-Pt system is about 1350°C compared to approximately 800°C for the equiatomic Fe-Pd composition. Because of the rapid ordering of the equiatomic Fe-Pt system during cooling it was found difficult to suppress and control the transformation during cooling even with a very rapid quench. Thus, an Fe-37at%Pt alloy rather than the equiatomic Fe-Pt composition was used for the Fe-Pt studies. The Fe-37at%Pt alloy composition can still be heat treated in the single-phase ordered region of the phase diagram over a large temperature range.

Figure 3 is a dark-field electron micrograph and corresponding electron diffraction pattern showing the small ordered regions in the disordered matrix of the as-quenched Fe-37at%Pt alloy. By monitoring the ordering process during the early stages of ordering in both the Fe-Pt and Fe-Pd alloys using X-ray diffraction and electron microscopy, it was concluded that the $A1 \rightarrow L1_o$ transformation at the aging temperatures studied (~ 500 - 700°C) occurs by a nucleation and growth process. Two distinct X-ray peaks corresponding to the ordered and disordered phases coexist from the earliest stages of the ordering process and the dark-field microscopy observations clearly reveal the formation of ordered particles within a disordered matrix. The X-ray and electron diffraction data also indicated that the

initial ordered, tetragonal precipitates ($L1_o$) exhibit a c/a ratio different than the final equilibrium value which gradually moves to the final value during the ordering process. This behavior is almost certainly the result of the coherency strains attendant to the transformation which are relaxed as the polytwinned structure emerges. During aging the ordered and disordered regions remain fully coherent until the disordered phase is finally consumed. Importantly, any one of the three <100> axes of the cubic phase can become the tetragonal c-axis of the $L1_o$ superstructure; hence, there are three possible variants of the tetragonal phase which can form within a single crystal or grain of the transforming parent cubic phase. The principal strains $\epsilon_1 = \epsilon_2 > 0$ and $\epsilon_3 < 0$ of the transformation give rise to appreciable shear components along the $\{110\}\langle 1\bar{1}0\rangle$ in the cubic matrix and Figure 4 shows the characteristic "tweed" contrast associated with these coherency strains [13]. The initial shape and habit of the incipient tetragonal particle have been somewhat controversial in the literature; however, careful analysis of the streaking in the electron diffraction patterns indicates that the ordered nuclei are small plates forming along the {110} planes of the cubic phase. These conclusions are supported by preliminary field-ion microscopy observations of the early stages of ordering. Furthermore, an elasticity theory of strain embryos and "tweed" in Fe-Pd alloys also indicates that the {110} habit is favored by the ordered particles during the early stages of transformations [14].

Figure 5 shows the characteristic alignment of the ordered particles along the {110} planes and <110> directions of the cubic matrix during the early stages of aging resulting from elastic interaction. Initially, all three variants of the ordered phase exist in a region of the transforming parent phase, but as the transformation proceeds two variants generally

emerge dominant apparently through stress-affected growth and coarsening producing alternating bands along the {110} planes comprised of orthogonal variants which are essentially twin-related. The interpenetrating incipient twin bands are depicted schematically in Figure 6 from Khachaturyan [5]. During prolonged aging the growing ordered particles within the bands impinge and coalesce to form the polytwinned structures as shown in Figure 7. The impingement and coalescence of the ordered particles produce a very high density of antiphase boundaries (APB's) within the twin plates as is evident in Figure 8. The high density of APB's appears to play a central role in the mechanism of coercivity controlling magnetization reversal as will be discussed below. When the twin bands or plates become conjugated along the {110} planes the tetragonality causes a mutual rotation of the c-axes to produce the coherent twin boundaries.

Within a grain of the transforming alloy, colonies or twin clusters with different combinations of the variants form and impinge. Within this array, a coarsening process occurs driven by the elastic strain and surface energy of the polytwinned composite producing large regions dominated by two variants. This coarsening process is analogous to what has been termed "discontinuous coarsening" in lamellar morphologies resulting from eutectoid or eutectic cellular phase separation [15]. Khachaturyan and coworkers at Rutgers have observed a similar process in their recent computer simulations of cubic → tetragonal ordering transformation which incorporate the influence of elastic strains [16].

B. Magnetic Domain Observations

The Lorentz microscopy studies made during the initial stages of this research program represent the first definitive and comprehensive electron optical observations of the

evolution of the magnetic domain structures characteristic of the polytwinned ferromagnets. The domain studies employed conventional Fresnel (out-of-focus) and Foucault (in-focus) modes of imaging to correlate the magnetic contrast effects with the underlying microstructure. Figure 9 reveals the magnetic domains in the as-quenched Fe-37at%Pt alloy using the Foucault in-focus method and the "tweed" contrast associated with incipient ordering is seen in the background. Figures 10a and b are Fresnel images of the domain walls in the equiatomic Fe-Pd alloy aged 3 hours at 500°C. The microstructure is a two-phase mixture consisting of ordered ($L1_o$) particles aligned along the <110> directions of a disordered matrix. The irregular domain walls in Figure 10 appear to exhibit properties more characteristic of the ferromagnetic disordered matrix phase since the apparent wall thickness is > 500 Å compared to 50 - 100 Å expected for the ordered $L1_o$ uniaxial phase. (Domain wall thickness generally was estimated using the extrapolation of the divergent wall half-width method). Within the domains of the two-phase mixtures a "ripple" contrast [17] is often observed reflecting the fine-scale modulation of the local magnetization within the emerging polytwinned (microtwin) structure. In Figure 11 crystallographically "frozen" domains are observed to forming on the emerging macrotwin boundaries in the transforming Fe-Pd alloy. In addition, "serpentine" domain configurations emerge during aging giving rise to the macrodomain walls which cut across the microtwins within a macrotwin plate as seen in Figure 12a and 12b. As the fully ordered polytwinned microstructure develops the serpentine domain configurations break-up at the macrotwin boundaries and produce an array of nearly parallel lenticular domains which terminate on the emerging macrotwin boundaries as revealed in Figure 13. In the fully ordered state the domain wall thickness

was found to be ~ 60 Å in good agreement with the calculated wall thickness $\delta = \pi\sqrt{A/K}$ of 50 - 100 Å for the uniaxial ordered phase in the Fe-Pd system (K ~ 2.7 x 10^7 ergs/cc).

After prolonged aging the polytwinned structure coarsens under the influence of the surface and strain energies of the twin aggregates and large regions dominated by two variants emerge as discussed previously. These large polytwinned plates are shown in Figure 14. The thin linear contrast striations (light and dark) reveal the microtwins boundaries and microtwin bands within the macrotwin plates. In Figure 14 four macrodomain walls are revealed in Lorentz microscopy using the Fresnel and Foucault methods; two are "frozen" on the macrotwin boundaries and two serrated walls are seen traversing the microtwin plates. Figure 15 shows a schematic analysis of the domain configurations revealed in Figure 14. The thin lines represent the microdomain boundaries which are coincident with the traces of the $(10\bar{1})$ and (001) microtwin boundaries; the thick lines are the macrotwin boundaries coincident with the traces of the so-called macrotwin boundaries along (110). The serrated or kinked walls are 180° macrodomains cutting across the array of microtwins within the macrotwin lamellae. This scheme of domain configurations is similar to those suggested in the Soviet literature [18]; however, in the present analysis the walls within the macrotwins are assumed to lie along the {100} planes of the $L1_o$ phase whereas in the previous work the walls are generally considered to lie on {110} planes. The crystallographically "frozen" macrotwin walls coincident with the macrotwin boundaries are predicted to be comprised of 90° or alternating 90° and 180° wall segments in the wall. It has been suggested that the walls in the microtwin/macrotwin composites will be a mixture of Néel and Bloch walls and future work will be directed at differentiating these wall

segments. The walls fixed by the crystallography of the microtwins, however, are expected to be 90° Bloch walls. The simple model of Figure 15 exhibits the salient features of the experimentally observed wall configurations. Magnetization reversal in these polytwinned ferromagnets can be expected to be controlled by the motion of the 180° macrodomain walls located within the macrotwin plates, as shown in Figure 16, followed by rotation. Indeed, preliminary in situ observation of the dynamics of wall motion reveals a jerky motion of these serrated 180° macrodomain walls in a changing magnetic field.

C. Magnetic Properties

1. Magnetic Hardening

The age hardening curves of equiatomic Fe-Pd alloy specimens aged at 500°C for three metallurgical states are shown in Figures 17a and b. The bulk alloys were coldworked (rolled) 70% and 90% and recrystallized (and homogenized) at 950°C prior to isothermal aging. The melt-spun ribbon was aged following solidification. All age hardening curves show a rapid magnetic hardening followed by a relatively broad plateau. The aging curve for the bulk alloy deformed 90% and annealed prior to age hardening shows a sharper maximum. All of the bulk materials were fully recrystallized and exhibited grain sizes of 30 μm (70% coldwork) and 25 μm (90% coldwork), respectively. The average grain size of the melt-spun ribbon was approximately 1 μm. A very interesting and important result in these age hardening experiments is that the melt-spun equiatomic Fe-Pd alloys exhibit a peak hardness of approximately double that of the bulk processed materials. Preliminary metallographic analysis of this effect indicates that the microstructural scales (microtwin and macrotwin sizes, etc.) are smaller in the rapidly-solidified ribbon and this microstructural

refinement is the most likely source of the enhanced magnetic hardening. (The finer microstructure results in a higher APB density within the polytwinned plates. See discussion below.) Figure 17c shows the age hardening curves of the Fe-37at%Pt alloy aged at 650°C. The finer-grained Fe-Pt alloys (70 μm) also develops a somewhat higher peak hardness than the coarser grained (100 μm) material. Clearly, these results indicate an influence of the grain size on the development of the polytwinned microstructures within the transforming grains. The formation of the polytwinned structure appears to involve a relaxation of strain energy at both long and short wavelengths relative to the grain diameter and thus the grain size influences the twin cluster size, thickness of the microtwin and macrotwin lamellae, and resultant APB density.

2. Mechanism of Coercivity

The mechanism of coercivity controlling the hysteresis behavior of the polytwinned Fe-Pt, Fe-Pd and Co-Pt family of alloys has most often been described in terms of a model which virtually ignores the salient features of the twinned structures. In particular, magnetization reversal has been attributed to wall pinning associated with a two-phase state comprised of ordered particles dispersed in a disordered matrix. The magnetic hardness is supposed to derive from the steep gradients in domain wall energy in moving from the disordered ferromagnetic matrix through the high anisotropy ordered particles [7]. However, wall pinning by antiphase boundaries (APB's) has been suggested as a source of magnetic hardness in the polytwinned ferromagnets although these ideas have somehow been lost in the Soviet literature [8-12]. Wall pinning by antiphase boundaries (APB's) has been discussed with regard to magnetic hardening in the classic Cu-Mn-Al Heusler alloy by

Lapworth and Jakubovics [19]. Based on the microstructural observations and Lorentz microscopy studies of the domain structures cited above, it is suggested here that APB pinning is the most likely source of magnetic hardness in the Fe-Pt, Fe-Pd and Co-Pt polytwinned alloys. Magnetization reversal appears to occur through the motion of 180° macrodomain walls within the faulted twin plates. A tentative model has been developed which is an extension of the previous APB model which appeared earlier in the Soviet literature referred to above but more explicitly incorporates the APB structure as well as allowing for thermally activated wall motion. This new model gives a better description of the temperature dependence of the coercivity and provides a microstructural basis for the difference between the coercivities attained in melt-spun Fe-Pd alloys compared to bulk alloys.

Consider a 180° macrodomain wall cutting across the microtwins in a macrotwin plate as shown in Figure 16. The quasi-rigid wall segment of area A generally moves under the influence of the externally applied magnetic field through a uniform magnetic medium characterized by an exchange constant A_1, uniaxial anisotropy constant K_1, and saturation magnetization M_1. This domain wall, however, will encounter the planar defects (APB's) and these disturbed regions will on average be assumed to occupy an area A' (or areal fraction $A_o = A'/A$) of the total wall area A. The planar defect is considered as a local variation in intrinsic properties and essentially exhibits values A_2, K_2 and M_2 characteristic of the disordered regions. The exchange parameter A_2 and saturation magnetization M_2 are taken to be essentially the same as in the ordered $L1_o$ structure, but the magnetocrystalline anisotropy K_2 of the disordered phase is quite different, viz. $K_2 << K_1$. (For Fe-Pt, Fe-Pd

and Co-Pt alloys $K_1 \sim 10^7 - 10^8$ ergs/cc and $K_2 \sim 10^4$ ergs/cc.) The migrating wall is assumed to be a Bloch wall of thickness $\delta = \pi\sqrt{A_1/K_1}$ and energy per unit area $\gamma_o = 4\sqrt{A_1 K_1}$. The thickness of the planar defect is taken to be $w << \delta$.

A simple approach to estimating the interaction energy between the migrating wall and the planar defect is to assume an angular distribution of spins through the wall and a corresponding variation in the local energy density within the wall structure. As a first approximation, the energy density profile of the Bloch wall along a direction x normal to the wall is taken as

$$E(x) = \frac{2\gamma_o}{\delta}\left(1 \pm \frac{2x}{\delta}\right) \tag{1}$$

where the sign convention is positive for $x < 0$ and negative for $x > 0$; γ_o is the total domain wall energy per unit area and δ is the wall thickness. If the thickness of the planar defects $w << \delta$, the faulted region can locate inside the wall and perturb the energy profile. If the faulted regions are taken as thin slabs with properties A_2, M_2 and K_2, then the presence of the planar defect lowers the total wall energy and the net interaction energy can be written as

$$\Delta E(x) = -w A_o E(x) \tag{2}$$

where $A_o = A_1/A$ is the areal fraction of the wall occupied by the faulted regions. $\Delta E(x)$ represents a local energy well and this interaction energy has a minimum at $x = 0$. To move the wall away from the potential wall the retarding force exerted by the defect must be overcome by the applied field. The maximum retarding force per unit area is given by

$$F = -\frac{\partial \Delta E(x)}{\partial x} = \frac{4 w A_o \gamma_o}{\delta^2} \qquad (3)$$

and the coercivity can be estimated from

$$2 H_c M_1 A = \frac{4 w A' \gamma_o}{\delta^2} \qquad (4)$$

or

$$2 H_c M_1 = \frac{4 w A_o \gamma_o}{\delta^2} \qquad (5)$$

where $2H_cMA$ is the total force exerted by the applied field on the migrating domain wall at the coercivity. Thus, the coercivity can be written as

$$H_c = \frac{8 w A_o}{\pi^2} A_1^{-1/2} K_1^{3/2} M_1^{-1} \qquad (6)$$

using the relations $\delta = \pi\sqrt{A_1/K_1}$ *and* $\gamma_o = 4\sqrt{A_1 K_1}$ for a uniaxial material. The microstructural parameter A_o is clearly related to the density of APB's within the twin plates. Inserting the values of A_1, K_1 and M_1 for the Fe-Pd and Fe-Pt systems and taking w = 4 x 10^{-8} cm, the theoretical values predicted by the APB pinning model are $H_c \sim 10^2 - 10^3$ Oe for the Fe-Pd alloys and $H_c \sim 10^3 - 10^4$ for the Fe-Pt alloys assuming $A_o \sim 0.1 - 1.0$. These predicted values of the coercivity are in good agreement with the range of experimental values reported in the literature.

Figures 18, 19 and 20 show the experimentally determined values of the normalized or reduced coercivities of the Fe-Pt, Fe-Pd and Co-Pt alloys as a function of temperature. Also shown are the theoretical curves predicted by Equation (6). The experimental values

show a steeper temperature dependence for the Fe-Pt and Co-Pt alloys than the theoretically predicted curve whereas the values for the Fe-Pd system appear to fit the theoretical values quite well. It must be pointed out, however, that the temperature dependence predicted by Equation (6) derives only from the temperature dependence of the intrinsic properties A_1, M_1 and K_1 and does not include thermally assisted wall motion. Using a simple approach discussed by Gaunt [20] as an estimate of the influence of thermally activated wall motion on the temperature dependence yields a modified expression for the coercivity as follows

$$H_c(T) = \frac{8 w A_o A_1^{-1/2} K_1^{3/2} M_1^{-1}}{\pi^2} - \frac{25 k_B T}{\delta M_1 A} \qquad (7)$$

Now the temperature dependence of the coercivity $H_c(T)$ in Equation (7) takes into account both the temperature dependence of the intrinsic properties and thermal activation. When applied to the data for the Fe-Pt and Co-Pt systems, Equation (7) is in excellent agreement with the experimental results if a value $A = D^2$ where D ~ 300-400 Å is assumed. The length D ~ 300 - 400 Å matches very well the scale of the microtwins in these polytwinned ferromagnets. The excellent agreement between the Fe-Pd data and the theoretical curve predicted by Equation (6) is taken to be fortuitous based on a lack of reliable data for this system. The temperature dependence of the intrinsic properties was fitted empirically to the data for the equiatomic Fe-Pt alloy. It is concluded here that an excellent first approximation to quantitatively describing the magnetic hardening in the polytwinned structures has been established. The detailed description of the energetics of the elementary thermally activated process involved in wall motion will be addressed in the next phase of

the work. The concept of "blistering" in Gaunt's treatment of "weak" pinning [21] represents an approach that might be elaborated and applied to the polytwinned alloys.

Publications (See Appendix)

"The Structure and Properties of Rapidly-Solidified Iron-Platinum and Iron-Palladium Alloys": B. Zhang and W.A. Soffa, IEEE Trans. Mag., 26 (5), 1388 (1990).

"The Formation of Polytwinned Structures in Fe-Pt and Fe-Pd Alloys": B. Zhang, M. Lelovic and W.A. Soffa, Scripta Met., 25, 1577 (1991).

"Microstructure and Domain Structure in Fe-Pt and Fe-Pd Polytwinned Alloys": B. Zhang and W.A. Soffa, IEEE Trans. Mag., November 1991 (in press).

"The Relationship Between Microstructure and Magnetic Properties in Polytwinned Ferromagnets": B. Zhang and W.A. Soffa, to be submitted to Acta Met., September/October 1991.

III. FUTURE STUDIES

The first 2½ years of this research program have yielded some interesting results and new perspectives with regard to the structure-property relationships in the polytwinned ferromagnets. In the next research grant period(s) the following issues will be emphasized:

(1) The fundamental basis for the enhanced coercivities exhibited by the melt-spun equiatomic Fe-Pd alloys compared to the bulk alloys will be investigated thoroughly. This will involve a quantitative comparison of the scale of the microtwins and APB density in the bulk alloys and melt-spun ribbon. Can the microstructure be sufficiently refined to change the essential features of the domain structure and mechanism of magnetization reversal?

(2) The initial Lorentz microscopy studies have been very encouraging. The domain work will be expanded significantly in the next phase of the research program. Preliminary in situ observations of wall motion suggest that more attention should be paid to dynamic observations.

(3) The APB pinning model will be elaborated and the energetics of thermally activated wall motion will be addressed more rigorously.

(4) A more quantitative approach to describing the APB density will be included in the electron microscopy studies. This quantitative metallography will provide an important component for evaluating the microstructural term in the description of the coercivity based on APB pinning.

IV. PERSONNEL

Three full-time graduate students will be affiliated with program over the next grant period. Below is a brief sketch of their academic backgrounds and status.

Mr. David P. Hoydick

Mr. Hoydick is a 1991 honors graduate of the University of Pittsburgh majoring in Engineering Physics. He is expected to work on this project for his doctoral studies in Materials Science.

Mr. Timothy J. Klemmer

Mr. Klemmer is a 1989 graduate of the Department of Materials Science and Engineering here at the University of Pittsburgh. He is expected to complete his Master's Degree during the current academic year and plans to continue on the project for his doctoral studies.

Mr. H. Okumura

Mr. Okumura completed his Master's Degree in Materials Science at Kyoto University in Japan in 1990 and is pursuing his doctoral studies in magnetic materials here at the University of Pittsburgh. He joined the research group in September 1990.

Thesis Completed:

"Phase Transformation and Interrelationship Between Microstructure, Domain Structure and Magnetic Properties in Polytwinned Fe-Pt and Fe-Pd Alloys", B. Zhang, Ph.D. Thesis, University of Pittsburgh, September 1991.

"Field-Ion Microscopy Studies of Ordering in Fe-Pd Alloys", Milan Lelovic, M.S. Thesis, University of Pittsburgh, December 1990.

V. REFERENCES

1. K. Watanabe and H. Masumoto: Trans. Japan Inst. Metals, 24 (9), 627 (1983).

2. L.M. Magat, A.S. Yermolenko, G.V. Ivanova, G.M. Makarova and Ya. S. Shur: Fiz. Metal. Metalloved, 26 (3), 511 (1968).

3. M. Hirabayashi, S. Weissman: Acta Met., 10, 25 (1962).

4. G. Hadjipanayis and P. Gaunt: J. Appl. Phys., 50 (3), 2358 (1978).

5. A.G. Khachaturyan, Theory of Structural Transformations in Solids, John Wiley and Sons, New York (1983).

6. A.L. Roitburd, Phase Transformations '87, p. 414, Institute of Metals, London (1988).

7. P. Gaunt: Phil. Mag., 13, 579 (1966).

8. N.N. Shchegoleva, L.M. Magat and Ya. S. Shur: Fiz. Metal. Metalloved, 34 (3), 163 (1972).

9. L.G. Onopriyenko: Fiz. Metal. Metalloved, 44 (1), 7 (1977).

10. G.S. Kandaurova, L.G. Onopriyenko and N.L. Vlasova: Fiz. Metal. Metalloved, 64 (6), 1061 (1987).

11. Ya. S. Shur, L.M. Magat, G.V. Ivanova, A.I. Mitsek, A.S. Yermolenko and O.A. Ivanov: Fiz. Metal. Metalloved, 26 (2), 241 (1968).

12. G.S. Kandaurova, L.G. Onoprieko and N.I. Sokolovskaya, Phys. Status Solidi (a), 73, 351 (1982).

13. L.E. Tanner: Phil. Mag., 14, 111 (1966).

14. S. Muto, R. Oshima and F.E. Fujita: Materials Science Forum 56-58, p. 65 (1990).

15. J.D. Livingston and J.W. Cahn: Acta Met., 22 495 (1974).

16. A. Khachaturyan, Private Communication.

17. H.W. Fuller and M.E. Hale: J. Appl. Phys., 31 (2), 238 (1960).

18. N.I. Vlasova, N.N. Shchegoleva and Ya. S. Shur: Fiz. Metal. Metalloved, 63 (3) 463 (1987).

19. A.J. Lapworth and J.P. Jakubovics: Phil. Mag., 24 253 (1973).

20. P. Gaunt: J. Appl. Phys., 43 (2), 637 (1972).

21. P. Gaunt: Phil. Mag., B48 (3), 261 (1983).

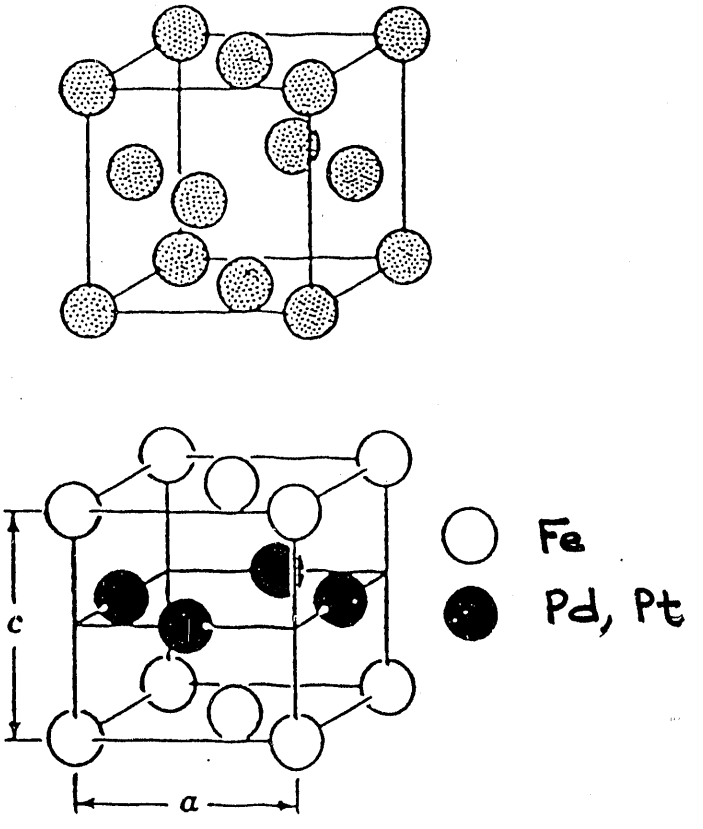

Figure 1 a) The unit cell of the disordered cubic A1 phase; b) the unit cell of the ordered tetragonal $L1_0$ phase.

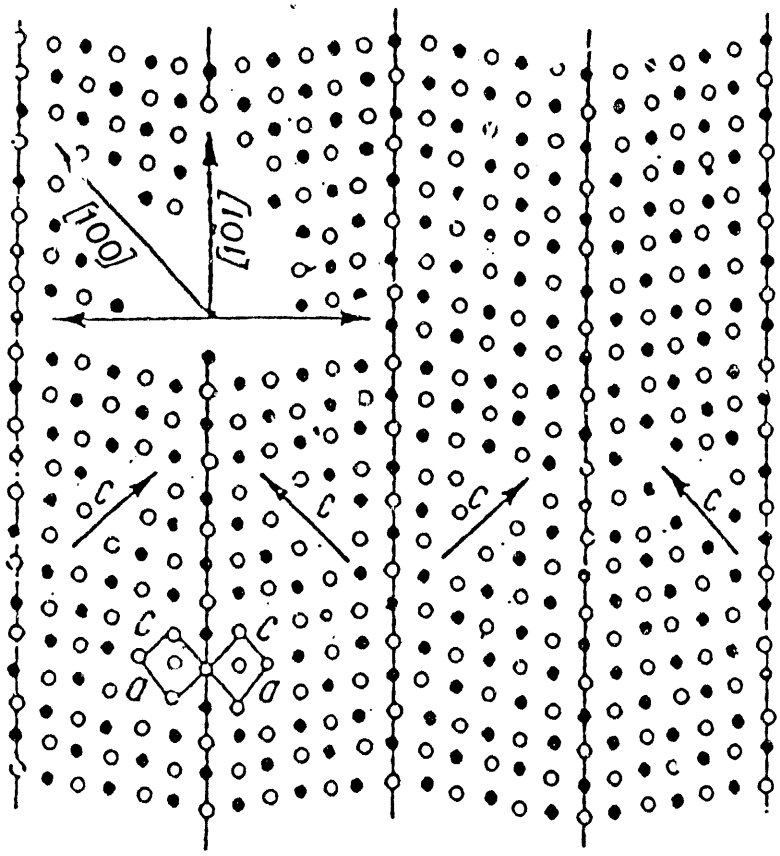

Figure 1 c) Model of the microtwins having strain-free twin boundaries and c-axes 88° apart in adjacent twin plates.

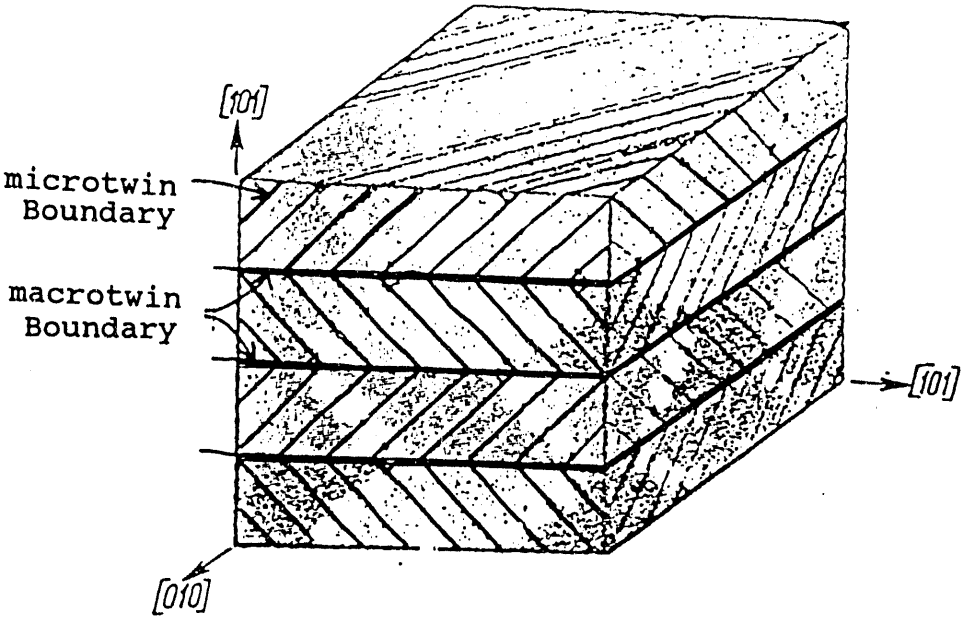

Figure 1 d) The ideal polytwinned structure, microtwins and macrotwins

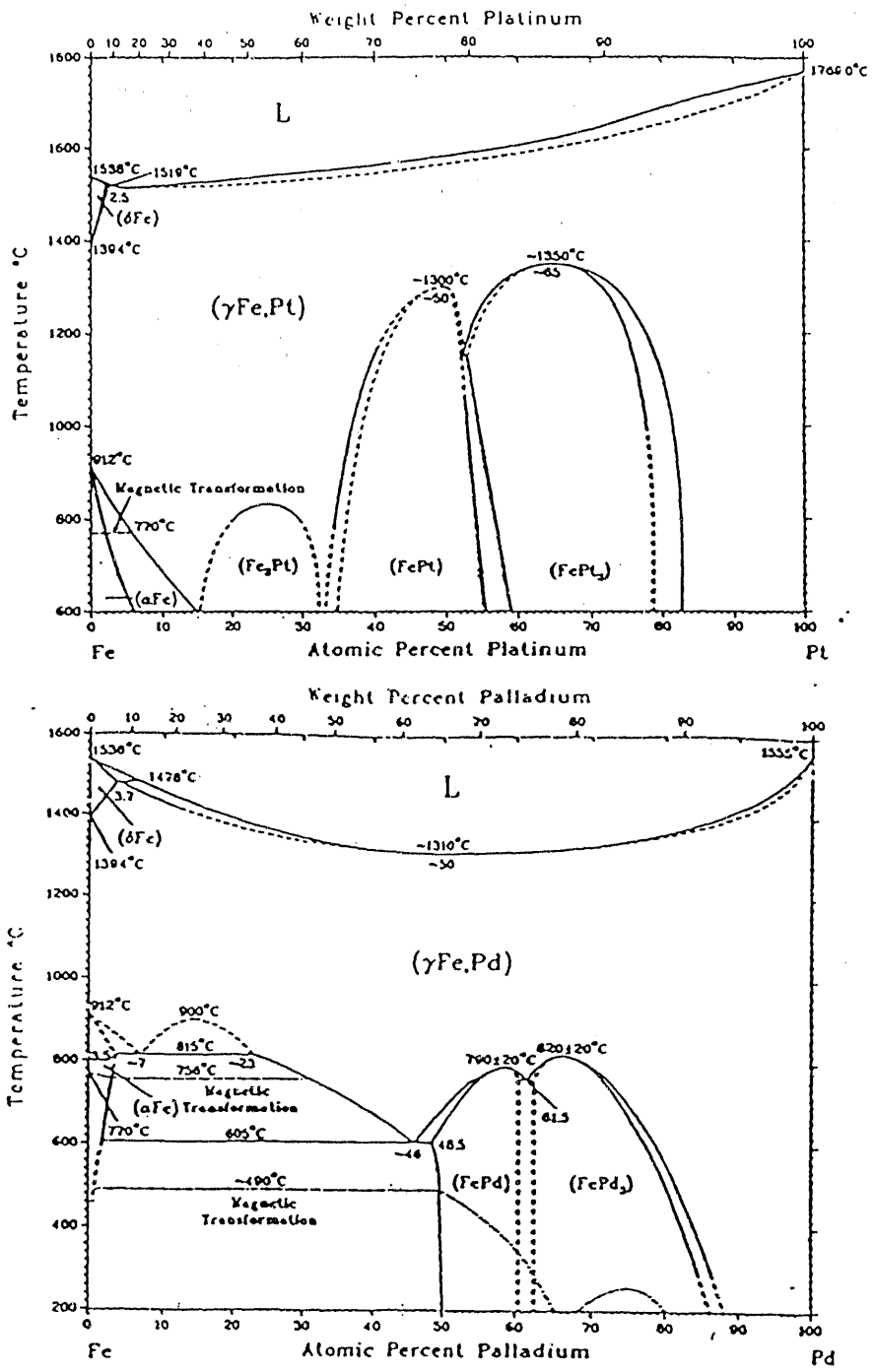

Figure 2 Phase diagrams of binary alloys a) Fe-Pt; b) Fe-Pd.

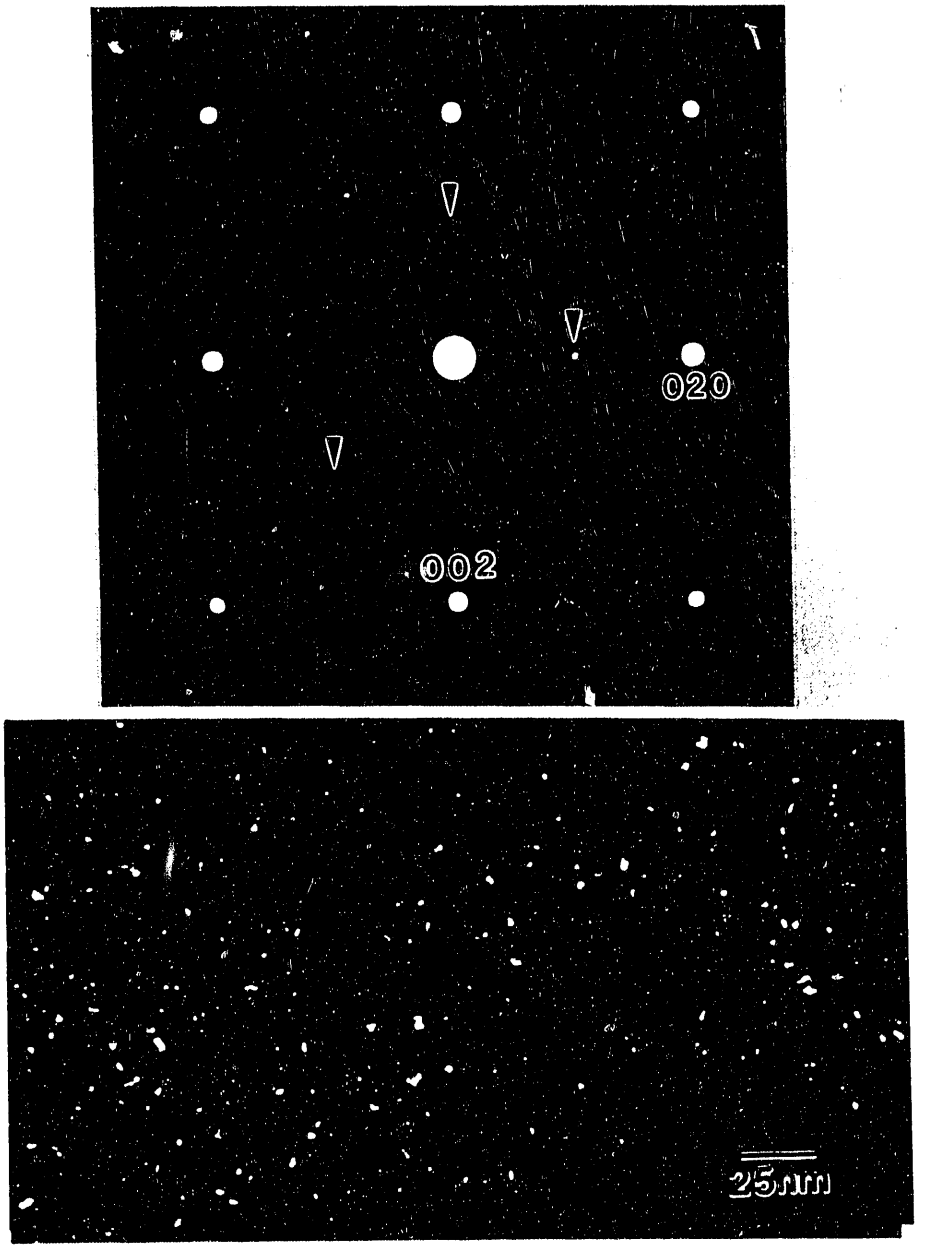

Figure 3 As-quenched Fe-Pt alloy: a) ($\bar{1}00$) zone diffraction pattern showing the superlattice reflections from the three variants; b) dark-field image showing the precipitates using one of the three (001) superlattice reflections.

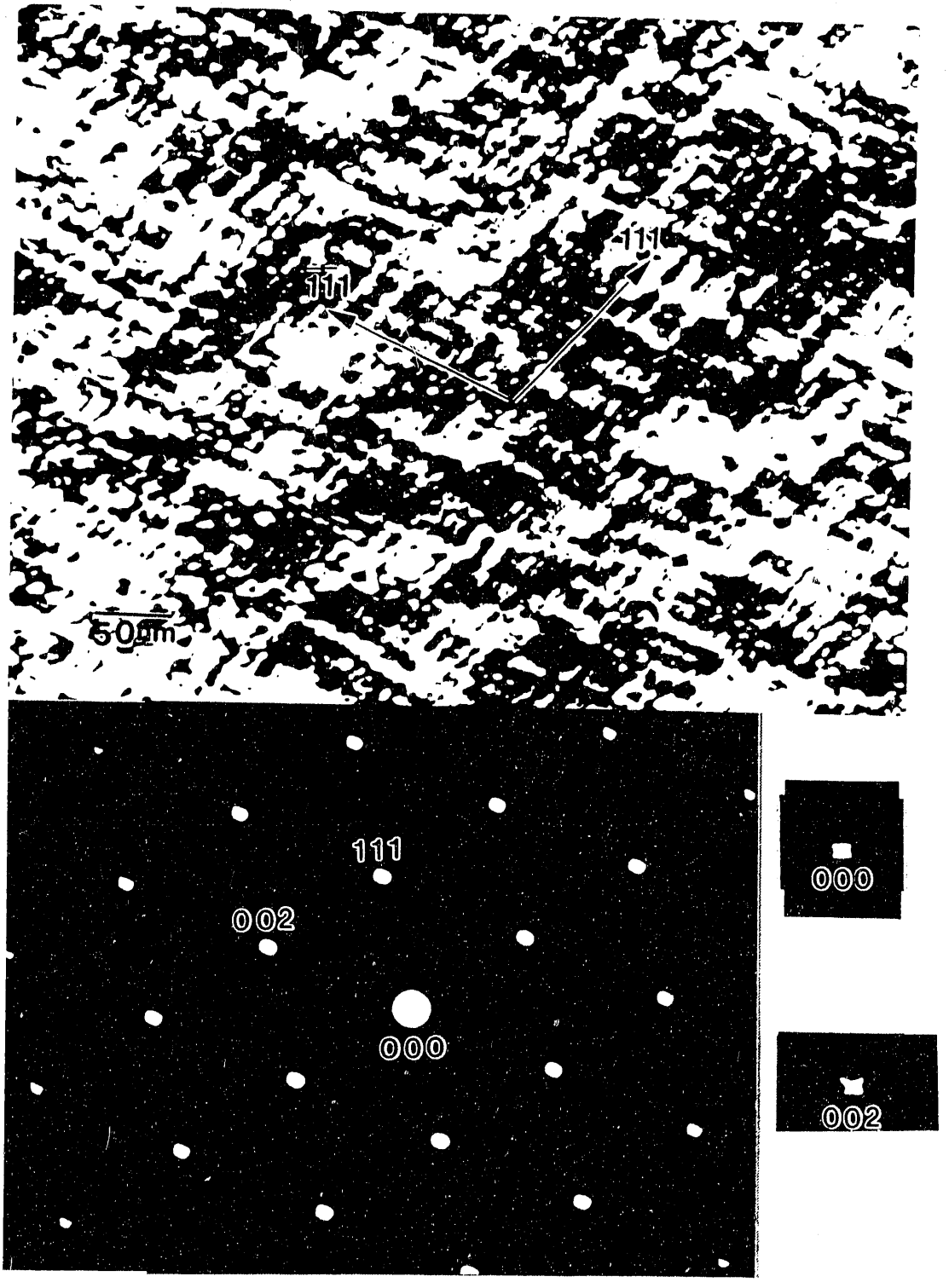

Figure 4 a) "Tweed" contrast under two beam condition; b) $(1\bar{1}0)$ zone diffraction pattern, the enlarged (000) and (002) spots showing <110> type streaking: Fe-Pd alloy aged 30 minutes at 500°C.

a)

b)

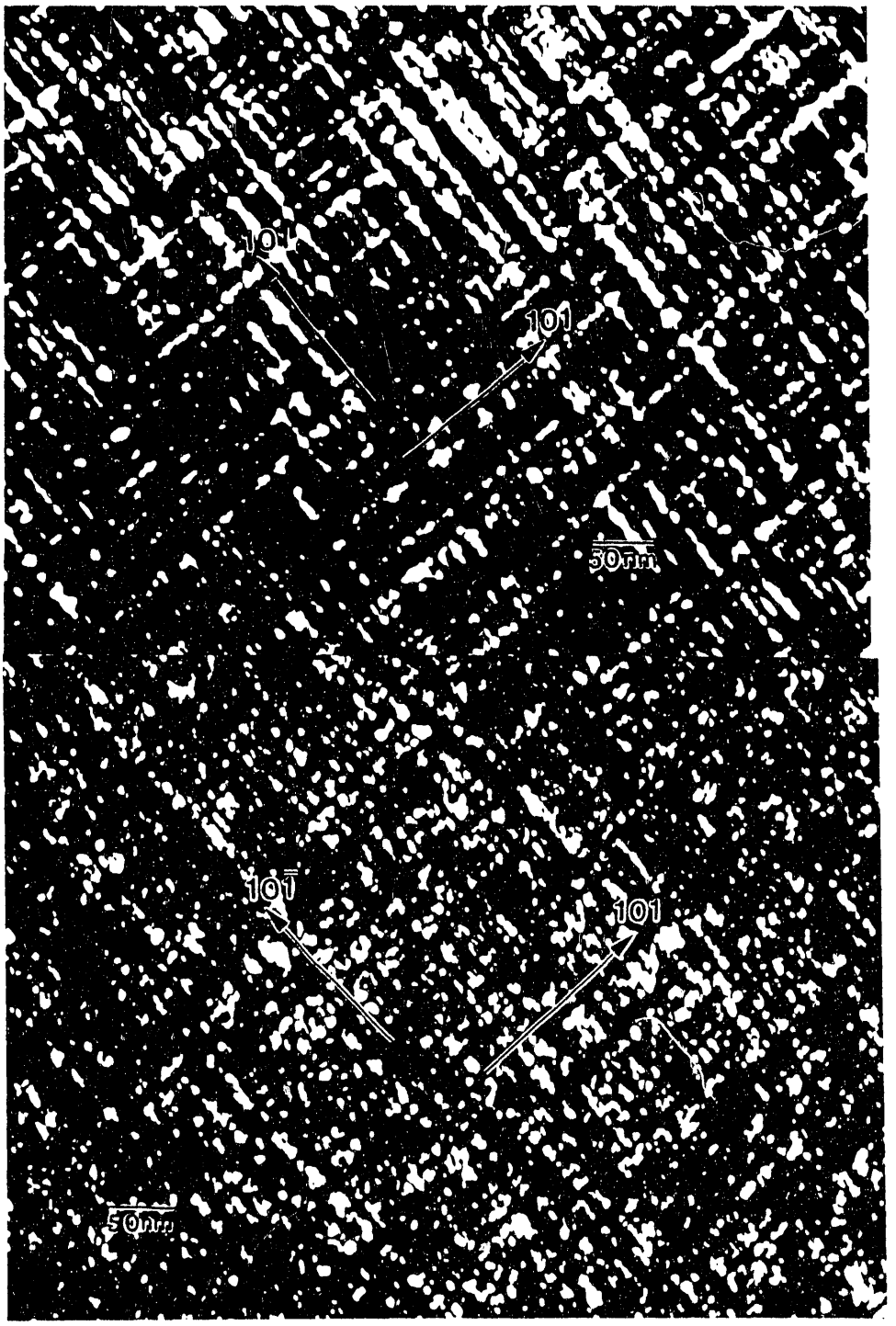

Figure 5 Dark-field images of Fe-Pd alloy aged 3 hours at 500°C: a) using $(001)_1$; b) using $(001)_2$.

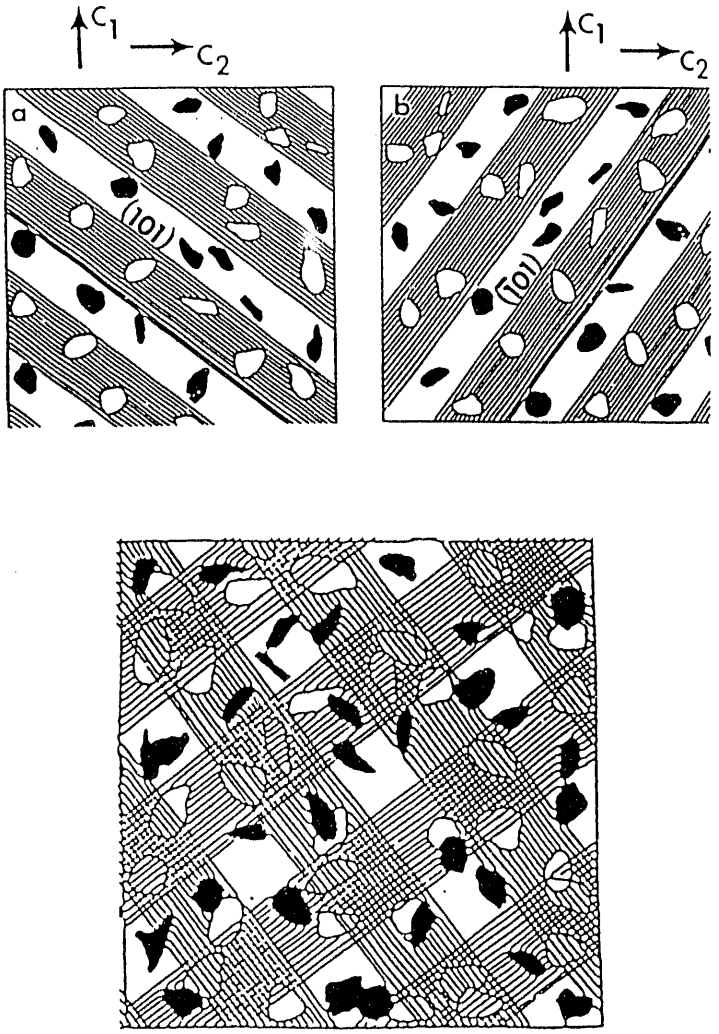

Figure 6 Schematic showing the distribution and alignment of tetragonal phase precipitates within alternating regularly spaced {110} bands (Khachaturyan): a) and b) are the two possible configurations of the bands lying on the (101) and ($\bar{1}$01) planes, respectively; the overlap of the two configurations will yield the contrast as shown in Figures 4.20 and 4.21.

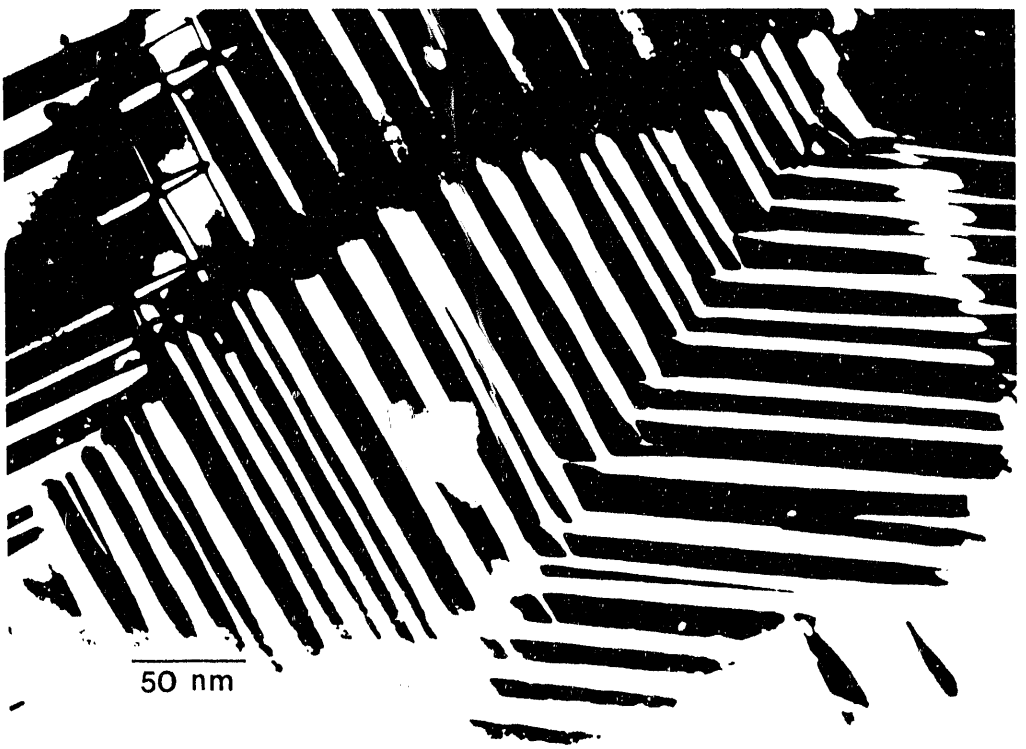

Figure 7 Macrotwins and macrotwin boundaries in an Fe-Pd alloy aged 61 hours.

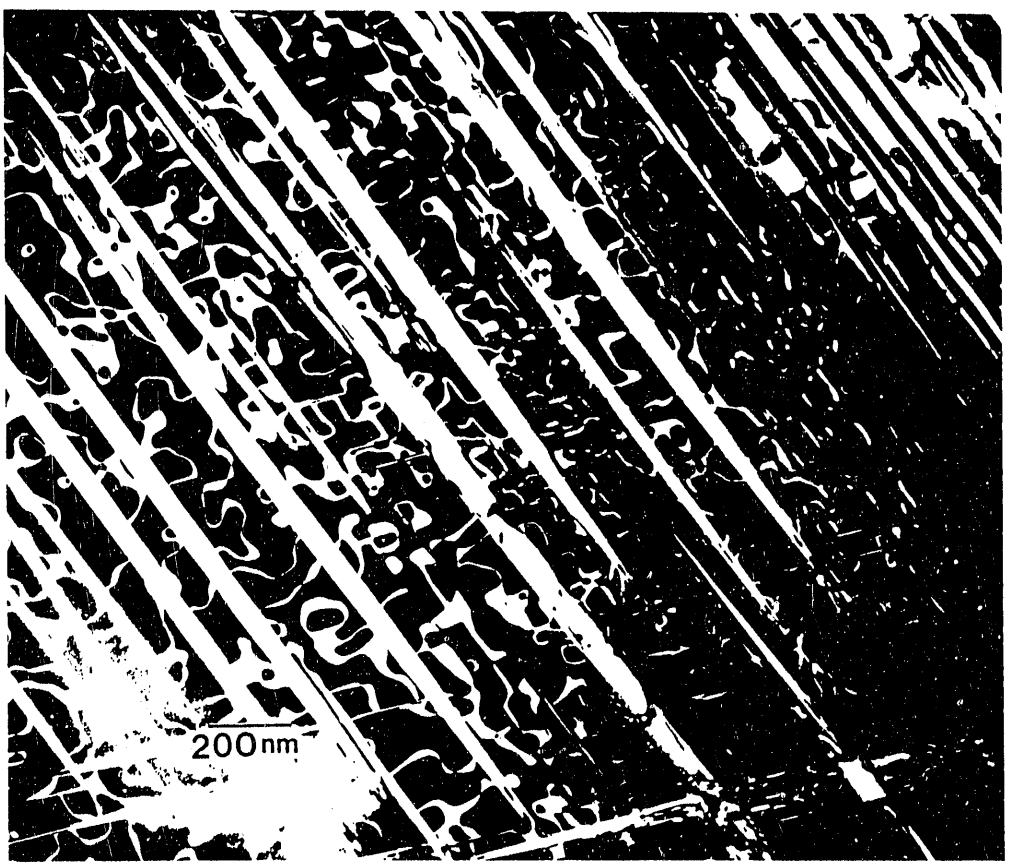

Figure 8 High density antiphase boundaries in an Fe-Pd alloy aged 61 hours.

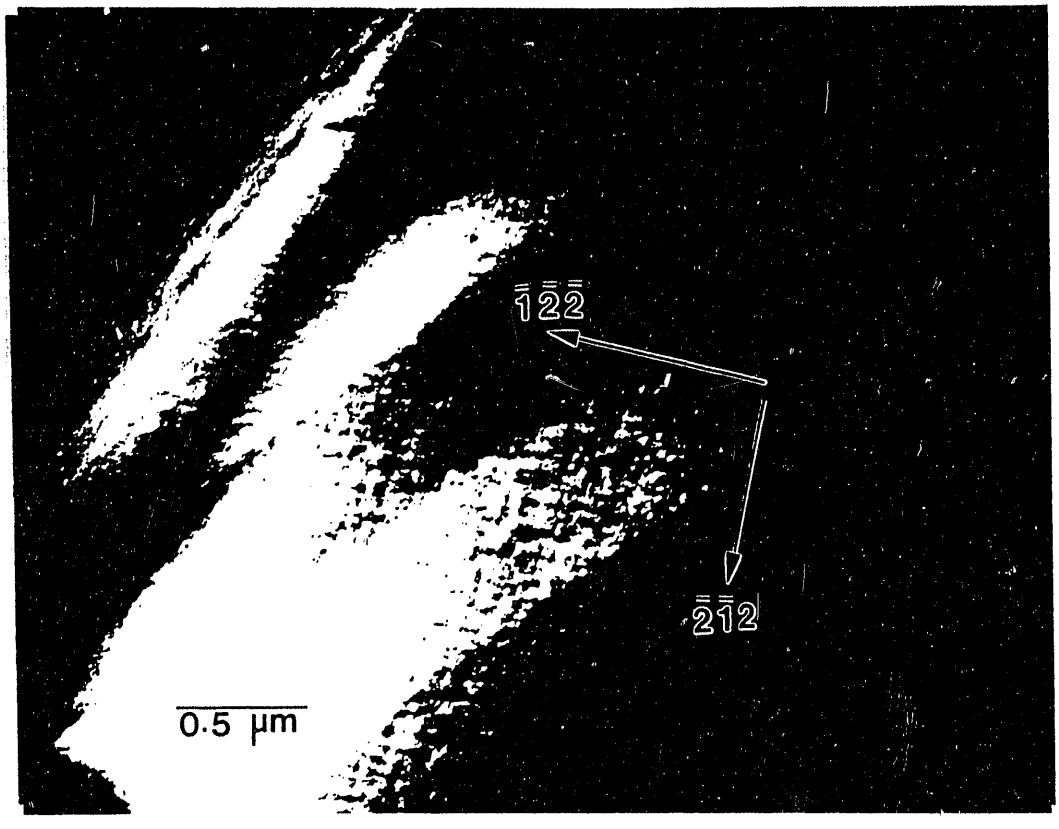

Figure 9 The "tweed" contrast and magnetic domains in an as-quenched Fe-37at.%Pt alloy, close to $(2\bar{2}1)$ zone (Foucault method).

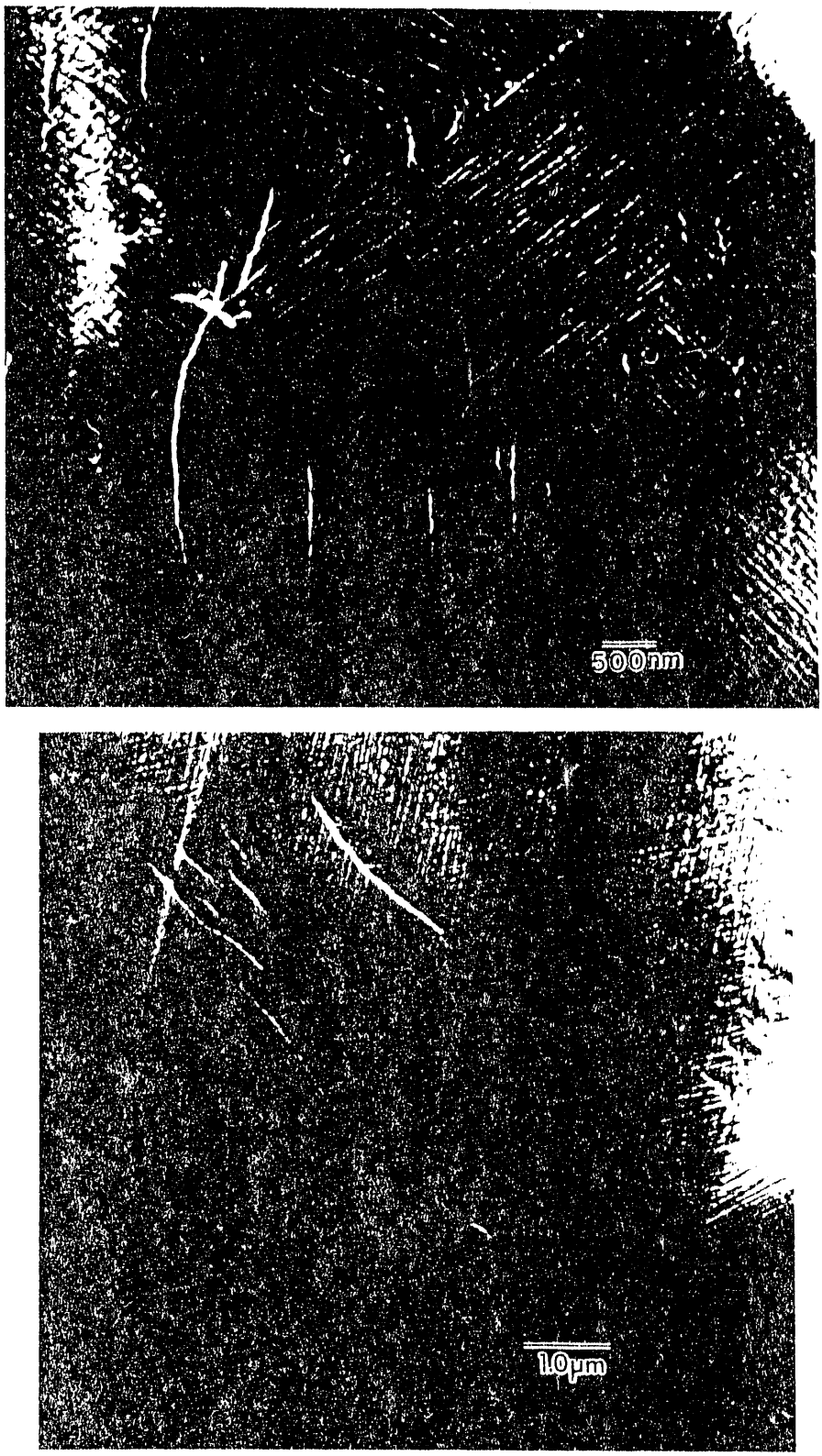

Figure 11 Irregular large domains and domain walls in the Fe-Pd alloy aged 3 hours (aging curve #1).

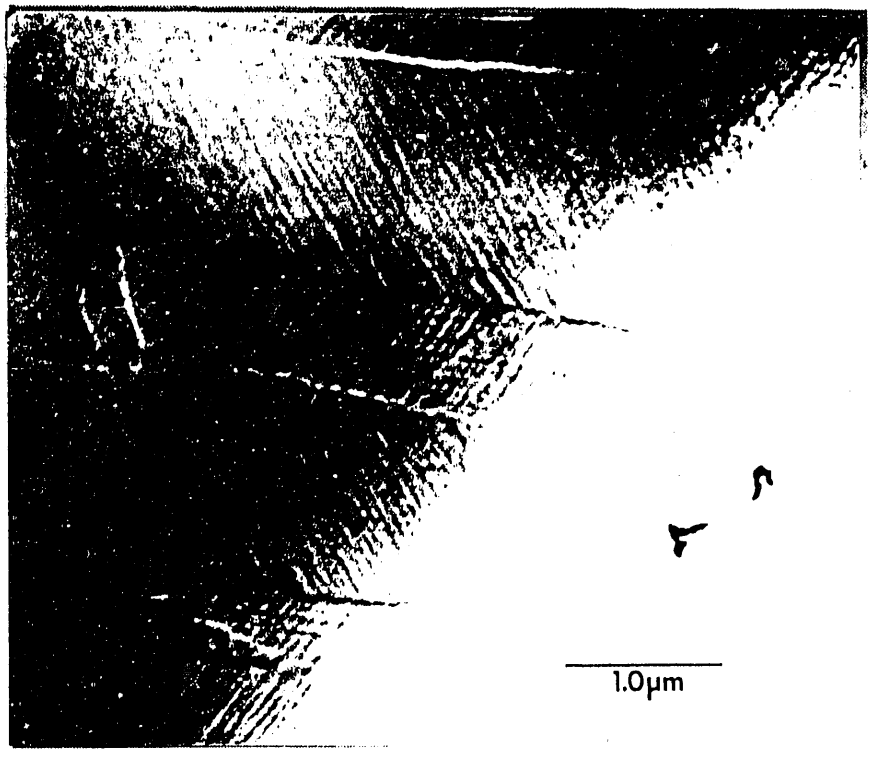

Figure 11 (a) Magnetic ripple contrast and the domain walls associated with the emerging twin cluster boundaries, Fe-Pd alloy aged 3 hours (aging curve #1).

Figure 12 Typical serpentine domains: (a) Fresnel over-focus; (b) Fresnel under-focus, in the Fe-Pd alloy aged 3 hours (aging curve #1).

Figure 13 (a) Lenticular domains in the peak hardness state: Fe-Pd alloy aged 5 hours (aging curve #2).

Figure 13 (b) Serpentine magnetic domains terminating on the twin cluster boundaries, close to the $(01\bar{1})$ zone: Fe-Pd alloy aged 3 hours (aging curve #1).

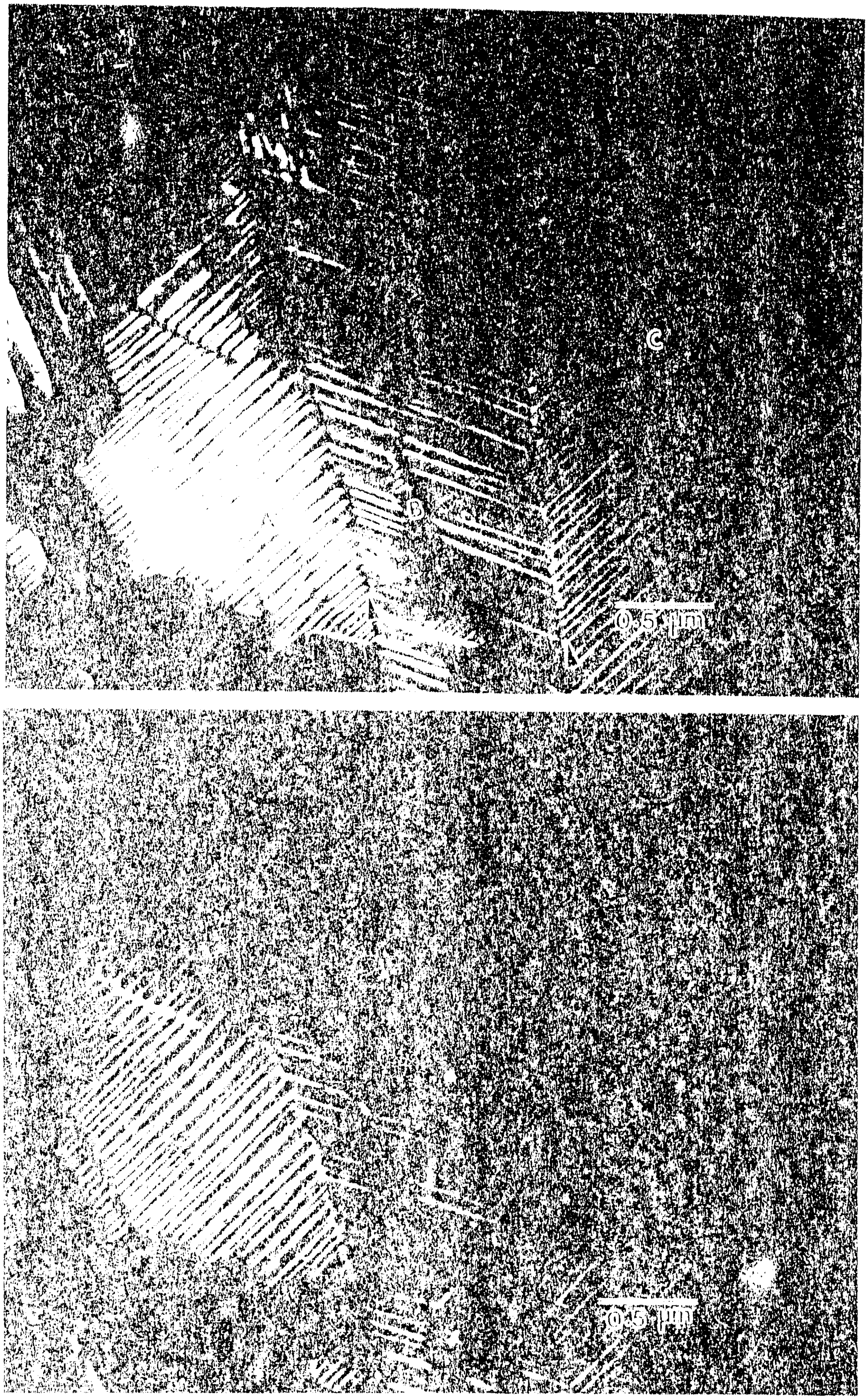

Microdomain and macrodomain structures and the domain walls: (a) Fresnel underfocus; (b) Fresnel overfocus; (c) and (d) Foucault in-focus images with the aperture displaced in opposite directions;

c)

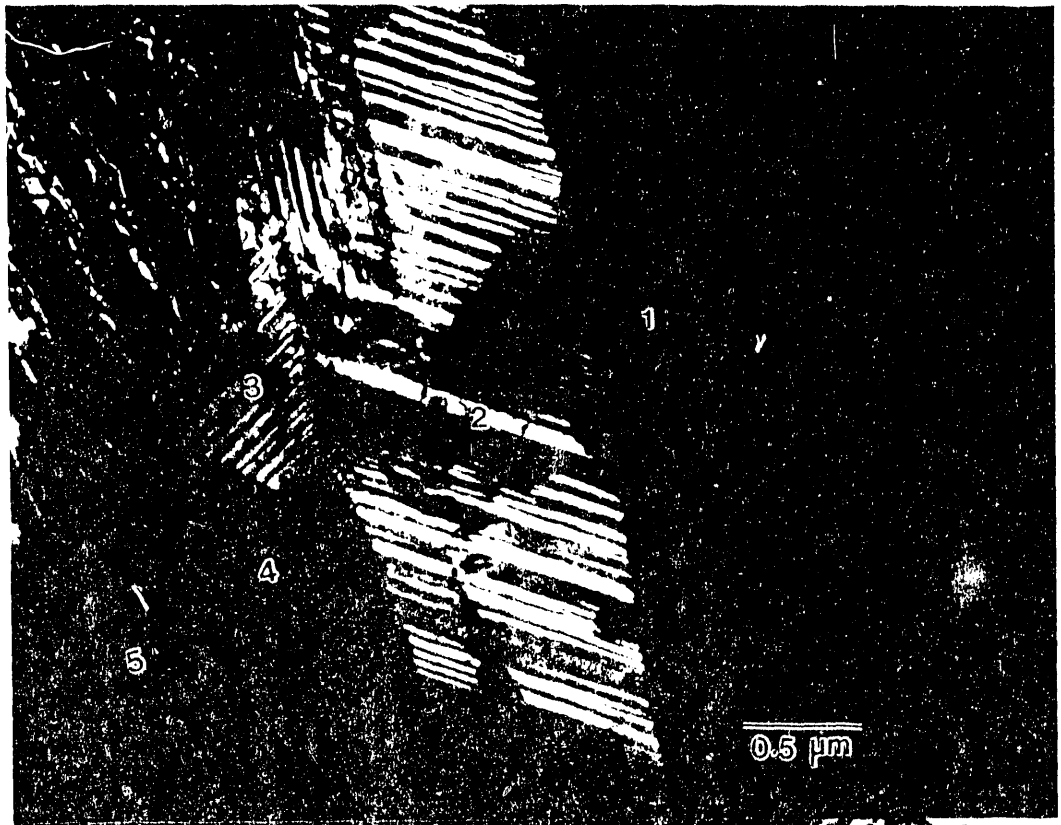

d)

Figure 14 (continued)

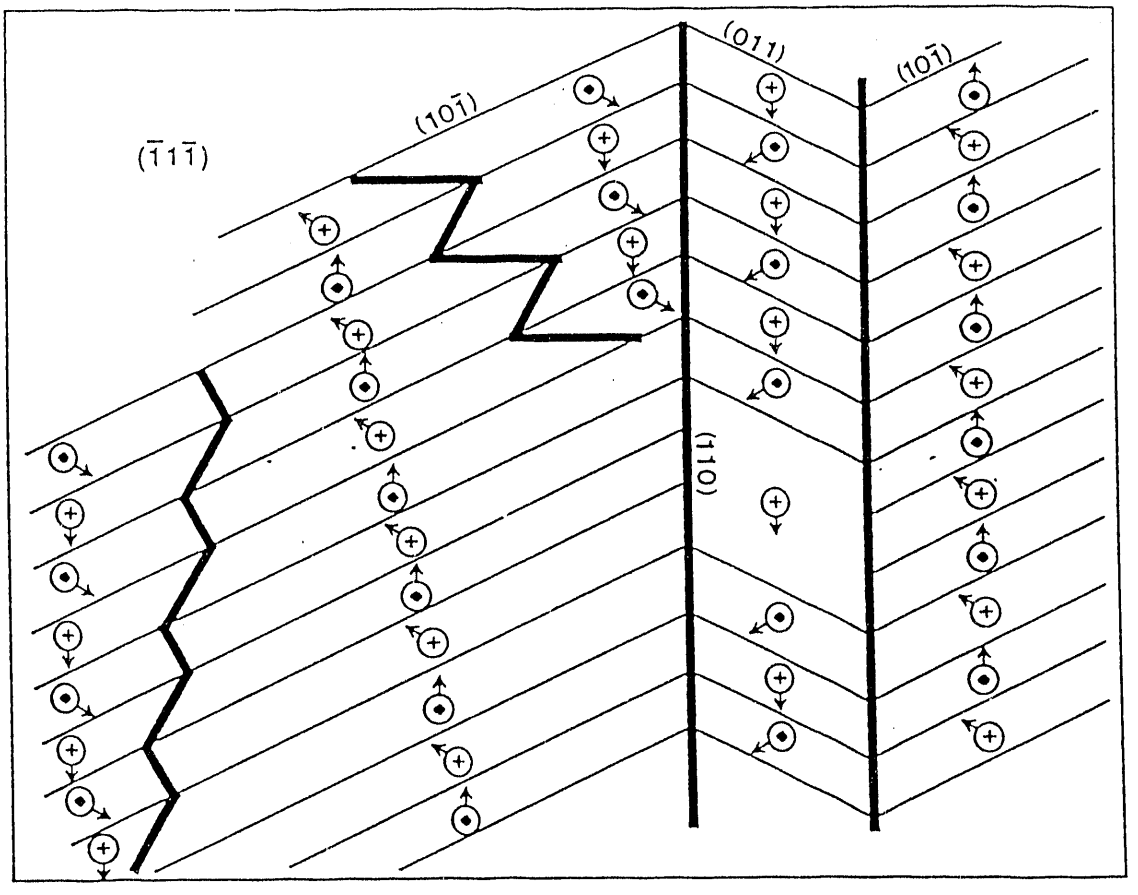

Figure 15 Schematic analysis of the domain configurations revealed in Figure 5.13 (the arrows represent the magnetization vectors inclined out of and into the plane of observation).

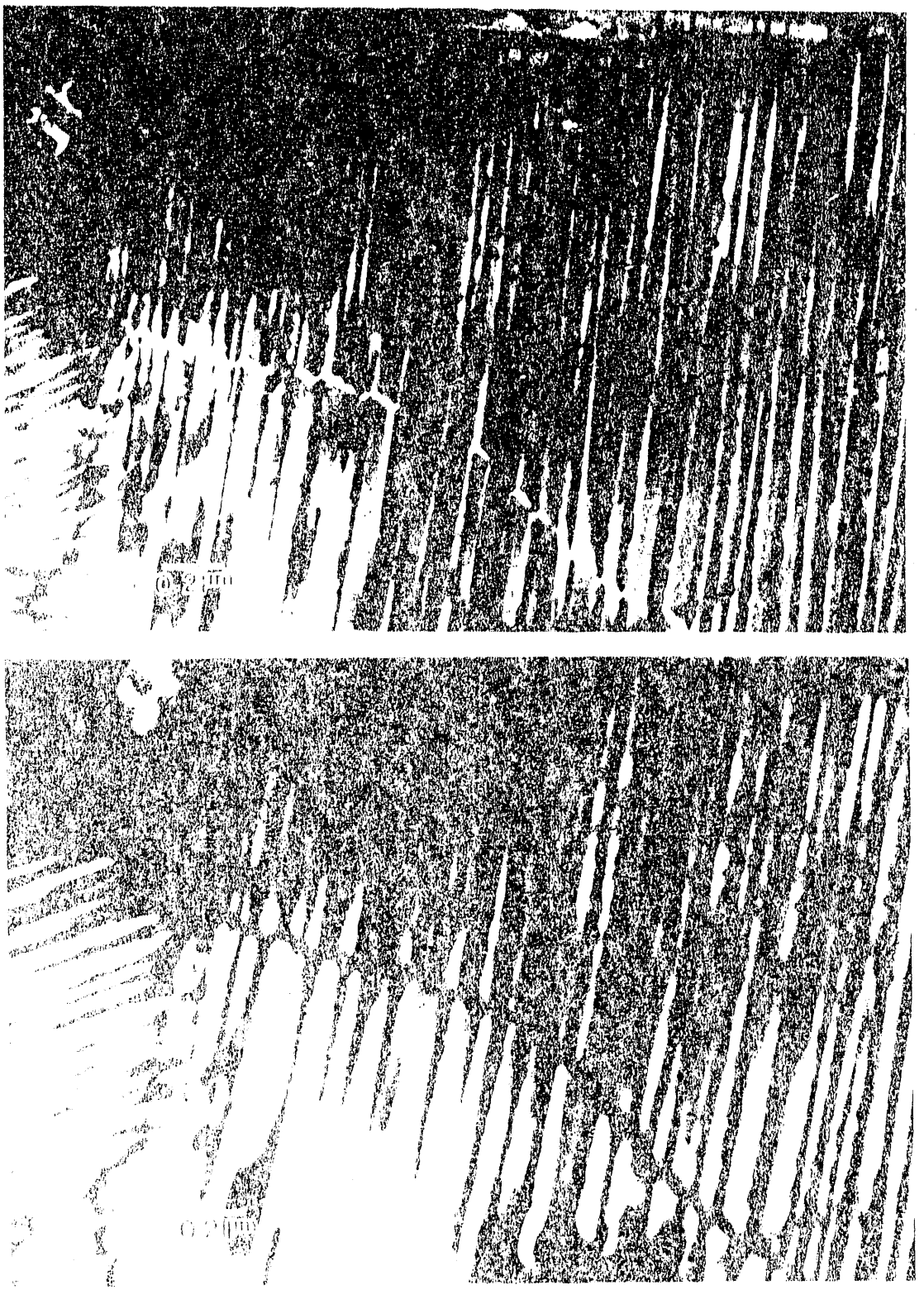

Bertodano walls cutting across the microtwin plates and showing the kinked features: (a) under focused condition; (b) over-focused condition; (c) and (d) in-focus Foucault images with the aperture displaced in opposite directions;

(c)

(d)

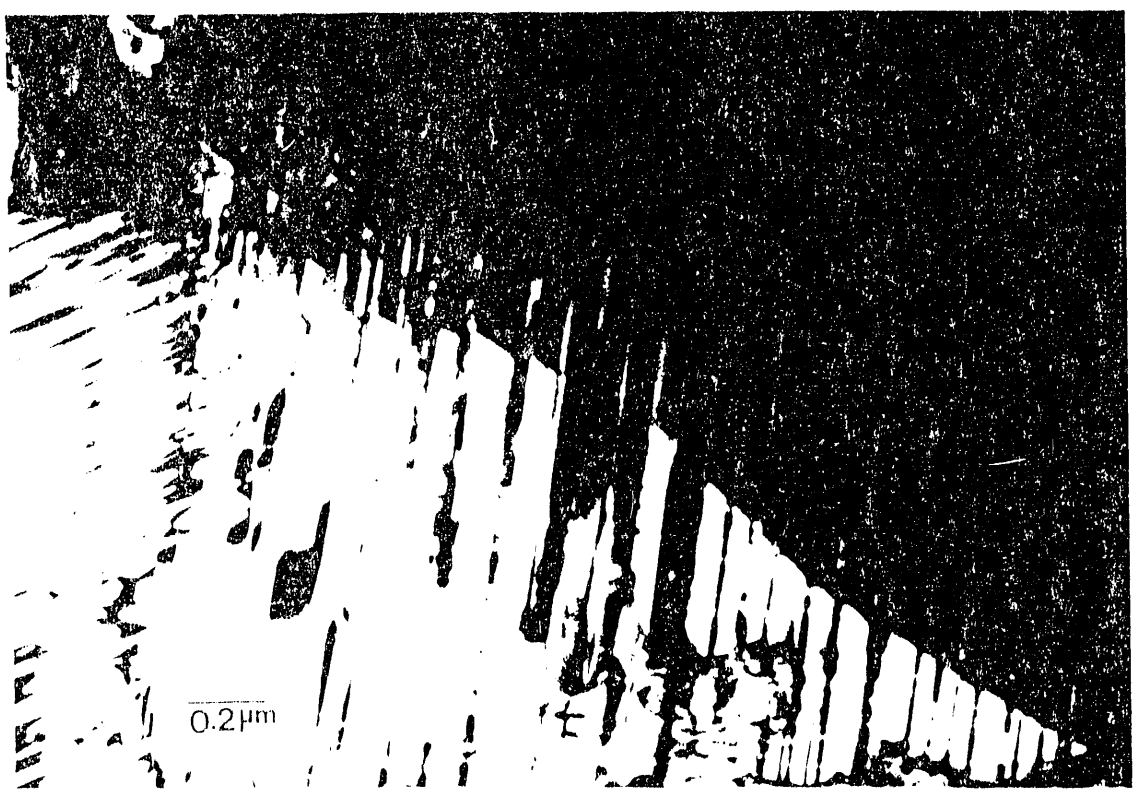

Figure 16 (Continued)

a)

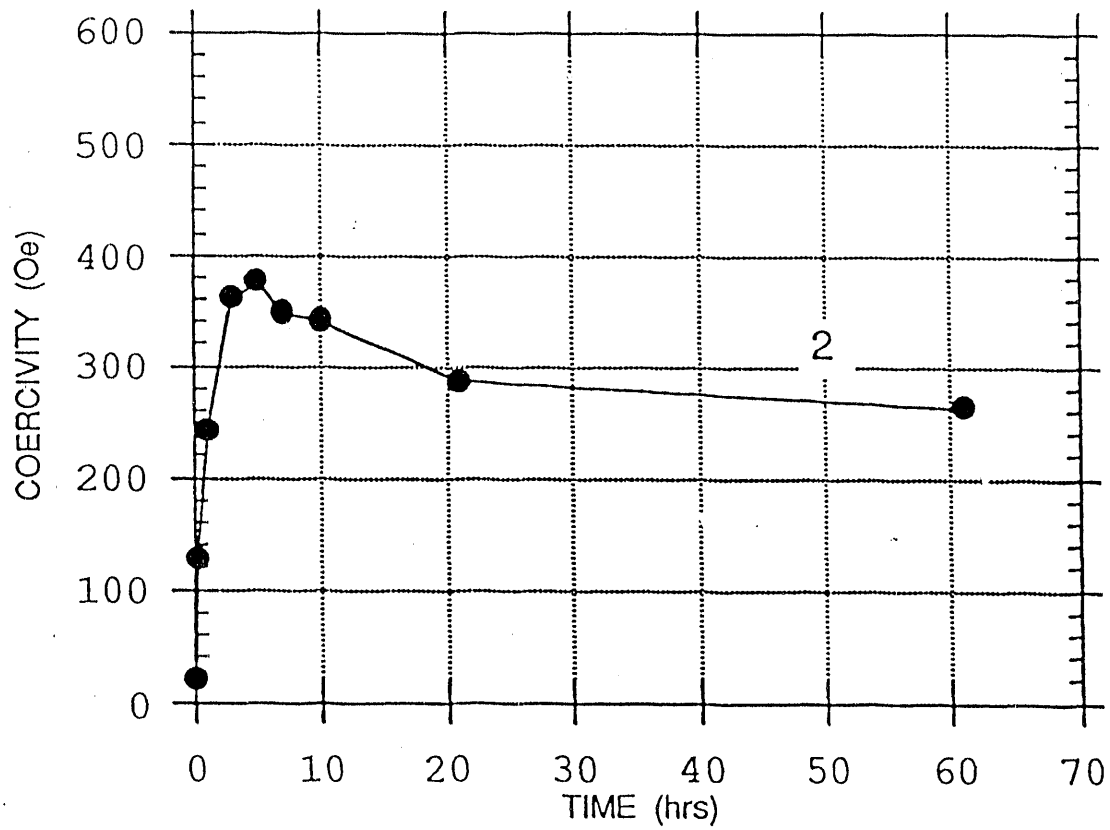

Figure 17 a) Aging curves of Fe-Pd alloys at 500°C, #1 curve from the bulk-alloy predeformed 70%; #3 curve from the melt-spun ribbon; #2 curve from the bulk-alloy predeformed 90%.

b)

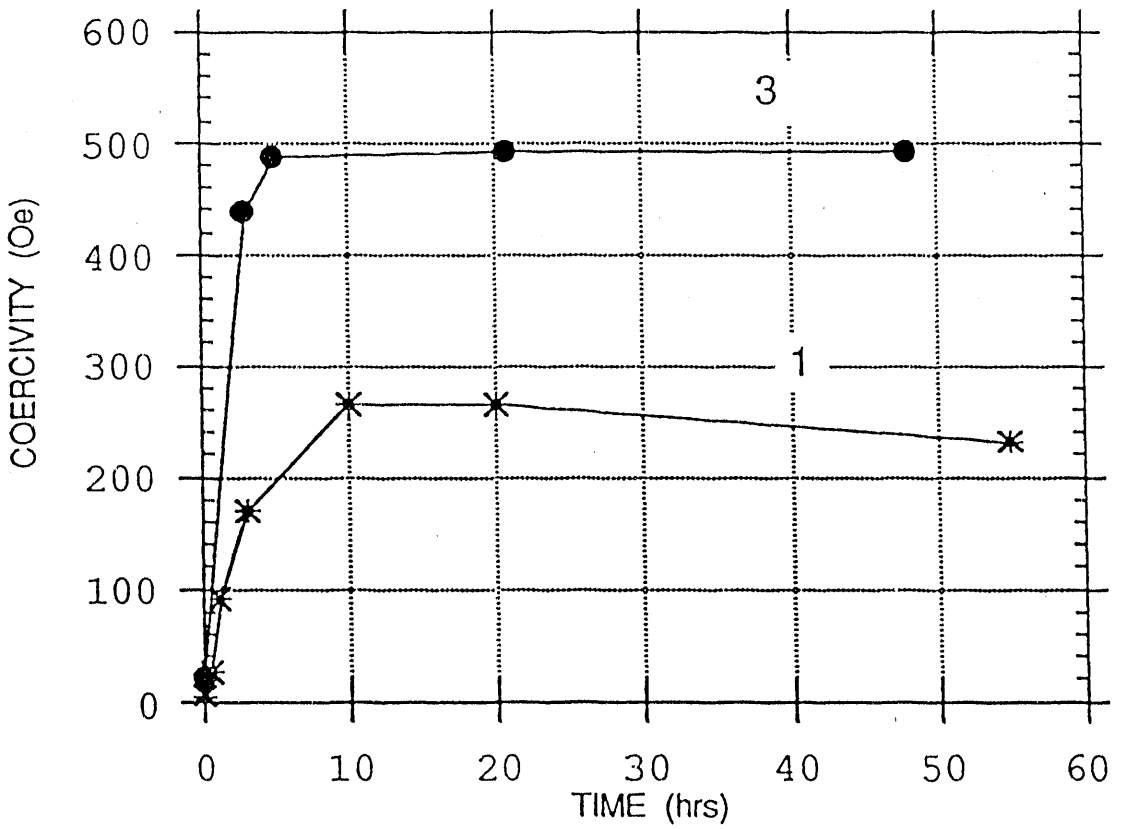

Figure 17 b) Aging curves of Fe-Pd alloys at 500°C, #1 curve from the bulk-alloy predeformed 70%; #3 curve from the melt-spun ribbon; #2 curve from the bulk-alloy predeformed 90%.

c)

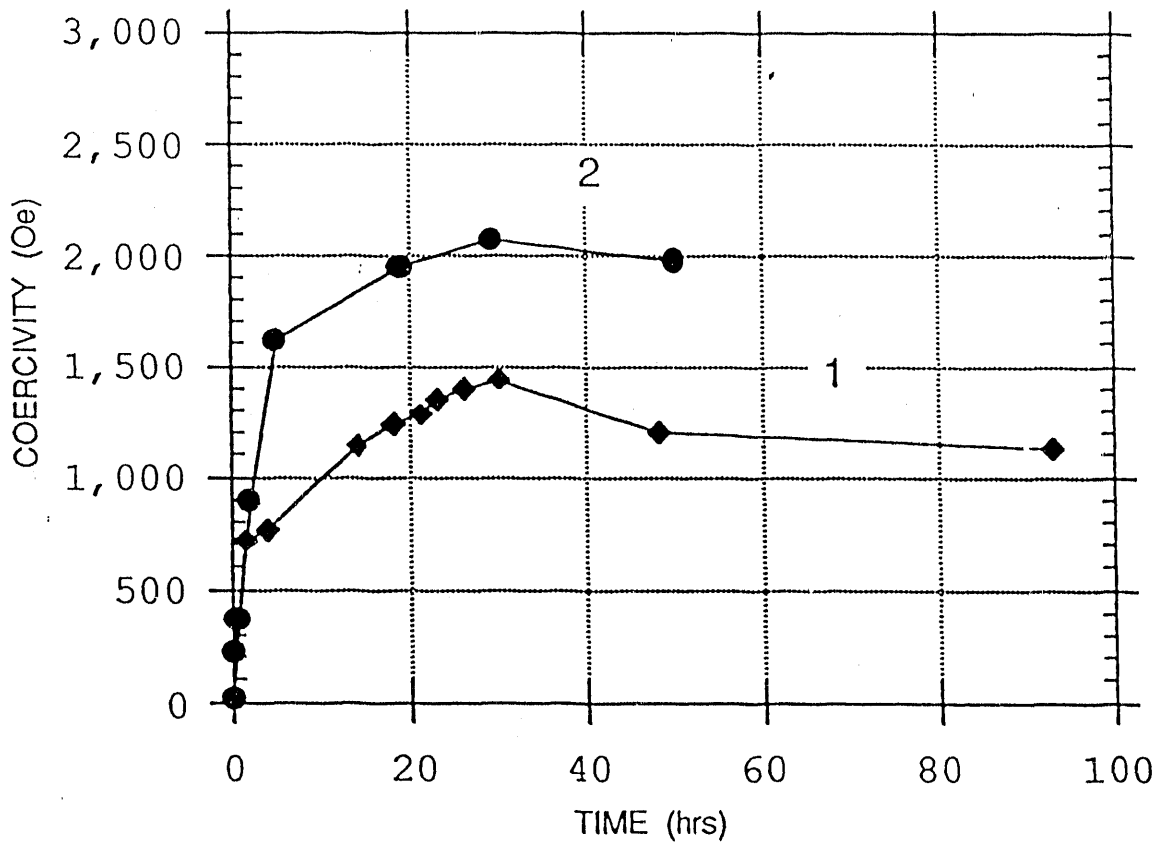

Figure 17 c) Age hardening curves of Fe-Pt alloys aged at 650°C, #1 curve from an alloy predeformed 70%; #2 curve from an alloy predeformed 90%.

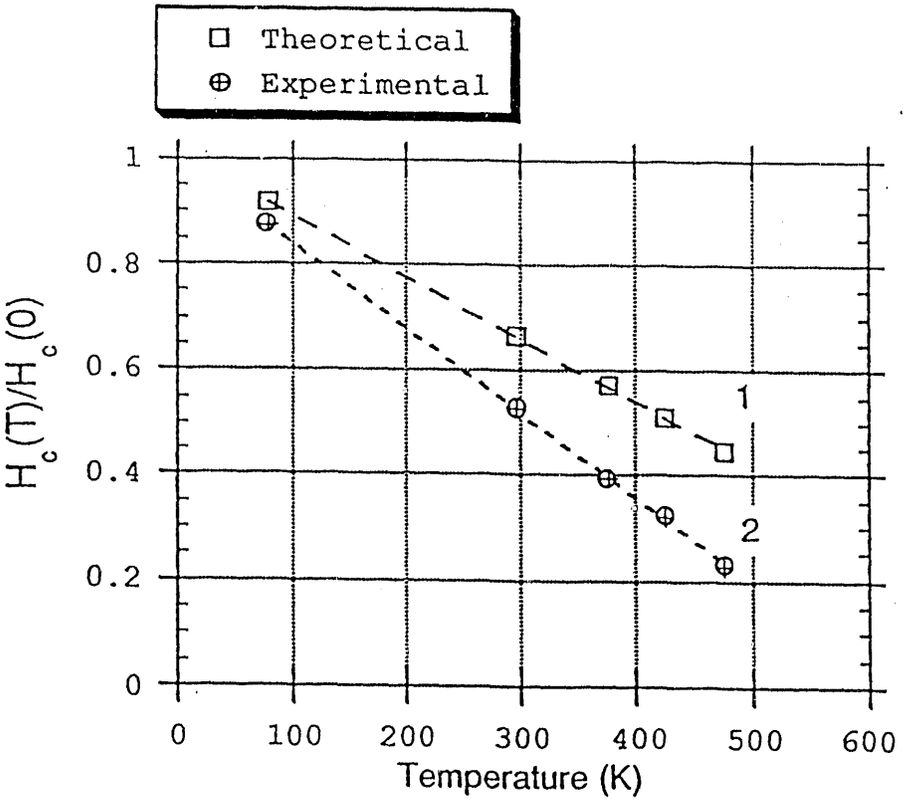

Figure 18 **The plots of the normalized coercivities versus temperature of the Fe-Pt alloy (theoretical (1) and experimental (2)).**

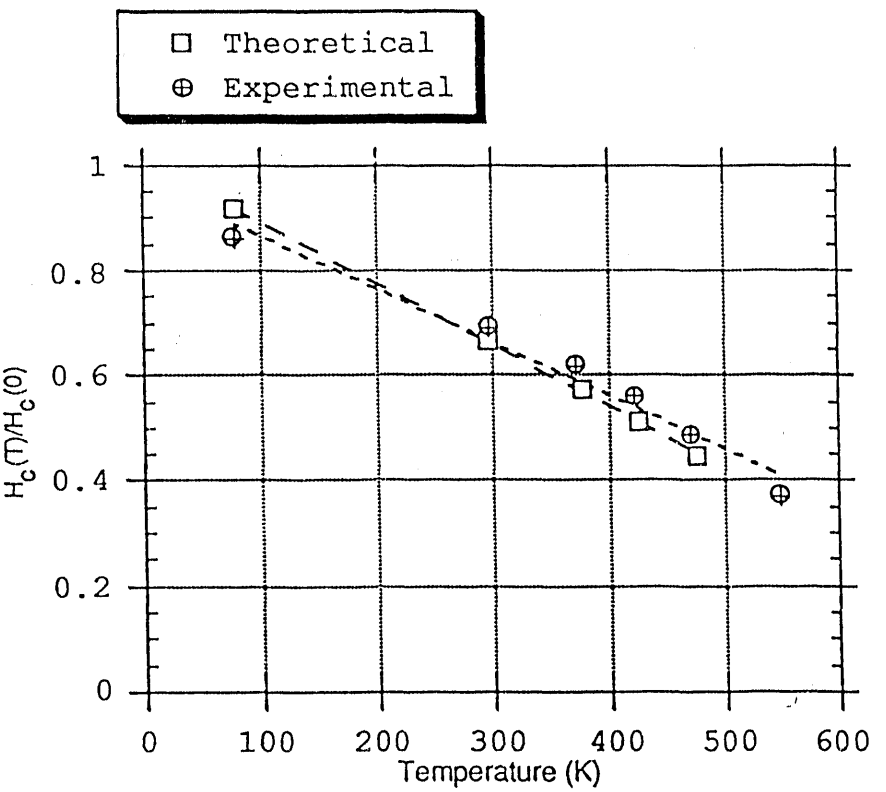

Figure 19 The plots of the normalized coercivities versus temperature of the Fe-Pd alloy (theoretical (1) and experimental (2)).

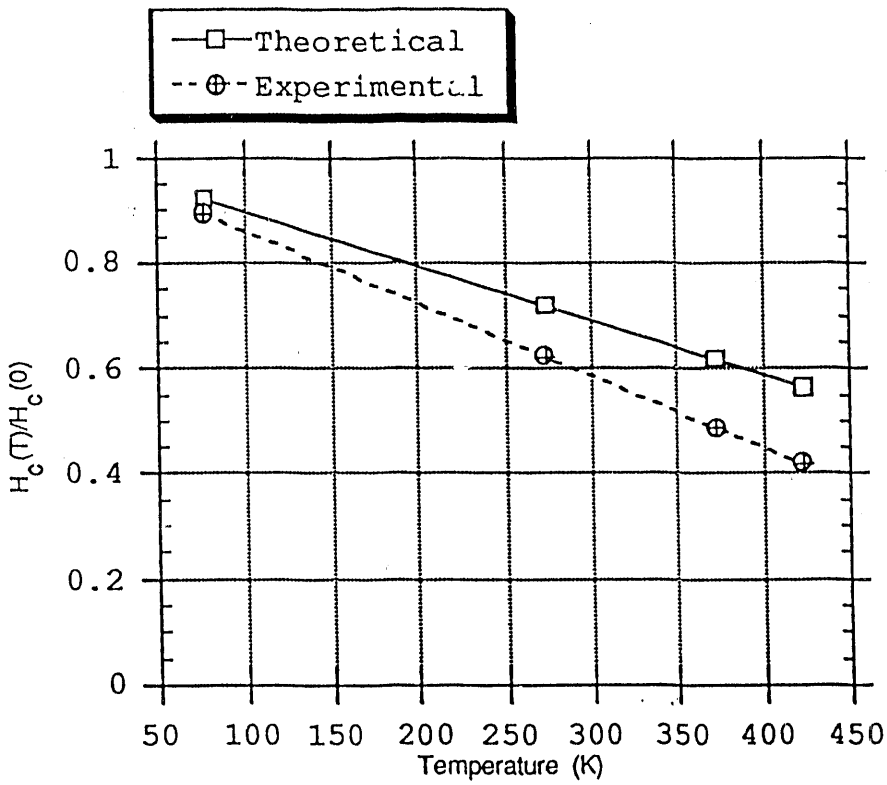

Figure 20 The plots of the normalized coercivities versus temperature of the Co-Pt alloy (theoretical and experimental).

APPENDIX

(Copyrighted papers removed)

DATE
FILMED
8/14/92